Robotica (2005) volume 23, pp. 149–158. © 2005 Cambridge University Press
doi:10.1017/S0263574704000669 Printed in the United Kingdom

Exploiting adaptable passive behaviour to influence natural dynamics applied to legged robots

Björn Verrelst*, Ronald Van Ham, Bram Vanderborght, Jimmy Vermeulen, Dirk Lefeber and Frank Daerden

Vrije Universiteit Brussel, Department of Mechanical Engineering, Pleinlaan 2, 1050 Brussels (Belgium)

(Received in Final Form: June 7, 2004)

SUMMARY

This paper reports on the use of a particular actuator in the field of legged robots. The proposed actuator, the Pleated Pneumatic Artificial Muscle, has some interesting characteristics which makes it suitable for machines which move by means of legs. An important issue is the actuator's adaptable passive behaviour which allows the stiffness of a joint that is actuated by two antagonistically coupled muscles, to be varied online. The natural frequency of the system can thus be changed in order to reduce control efforts and energy consumption. The idea of changing this natural frequency in combination with trajectory control will be implemented on a two-dimensional leg model. It will be shown that an appropriate choice of compliance can strongly reduce the amount of needed control activity and energy consumption while tracking a given trajectory.

KEYWORDS: Legged robots; Pneumatic artificial muscle; Passive/Active control.

I. INTRODUCTION

I.1. Legged locomotion and natural dynamics

In the last two decades, substantial progress has been made in the field of legged robots. One of the important and astonishing events happened in Tokyo on December 20th in 1996 when Honda Motor Corporation presented there first humanoid "Honda Human Robot"[1] after ten years of secret research. This autonomous humanoid is able to walk smoothly on level ground and even to climb stairs. In the next ten years the number of simular and even improved models increased rapidly, especially in Japan. Sony brought to the marked the dog pet-robot AIBO and recently they showed the "First Running Robot: QRIO"[2] which belongs to the family of small humanoid robots SDR4X-Sony Dream Robot.[3] For a few years the Japanese government together with most of the leading Japanese manufacturers have invested heavily in the HRP-project.[4] This project tries to create ready-to-use industrial, domotic and healthcare applications for humanoid robots. Most of the interest and development comes from Japan, but the USA and Europe have joined in although at different pace. In Germany the state of the art humanoid "Johnnie"[5] has been built, while in the USA NASA is working on the first "Robonaut"[6] for space applications.

These examples show that legged robots are no longer only futuristic elements for science fiction movies but that they will become a full part of technological evolution. In spite of the magnificent models already created, this evolution has, however, just began. A dextrous, intelligent, fast and fully autonomous humanoid robot is still far-off. A lot of research in many different fields, ranging from artificial intelligence to mechanical design, is to be done. One of the topics is the implementation of alternative actuators replacing the widely spread electrical drives, in order to make lightweight structures and compliant joints. The compliance characteristics can be used to reduce shocks and decrease energy consumption by exploiting the natural dynamics of the system.

Legged locomotion can be classified in terms of their overall control strategy. The more recent robots are dynamically balanced machines, whereas the older machines were statically balanced. Statically balanced robots keep the center of mass within the polygon of support in order to maintain postural stability. To avoid inertial effects these machines move rather slowly, contrary to dynamically balanced robots where the inertial effects are taken into account in the different control strategies. When the control unit not only takes these inertial effects into account but also exploits them, the term natural dynamics arises.

Natural dynamics or passive dynamics is the unforced response of a system under a set of initial conditions. In general, for legged locomotion these natural dynamics are not or only partially exploited. Examples of exploitation of the natural dynamics are the swing-leg swinging freely without hip actuation or the body, and stance-leg pivoting as an inverted pendulum around an unactuated ankle. Legged systems that walk completely without actuation are called "Passive Walkers". These machines are only powered by gravity and they are mechanically tuned in order to walk down a sloped surface. These "Passive Walkers" could be shown to be very energy efficient but unfortunately they are of little practical use. A minimum actuation should be provided to walk on level ground to overcome friction and impact losses. Anyway, it is important to exploit the natural dynamics by trying to incorporate the unforced motion of

* Corresponding author. E-mail: bjorn.verrelst@vub.ac.be. Website: http://lucy.vub.ac.be

https://doi.org/10.1017/S0263574704000669 Published online by Cambridge University Press

a system instead of ignoring or avoiding it. Doing so could positively affect energy consumption and control efforts.

One of the first to incorporate passive dynamics for legged locomotion was Matsuoko,[7] and later Raibert.[8] The latter became one of the pioneers in dynamic walking with his several one or more legged hopping robots. For these systems he used a pneumatic spring in the telescopic legs to influence and exploit the passive dynamics in the vertical direction. Exploiting passive dynamics by means of the stance leg pivoting freely as an inverted pendulum was incorporated in the biped walkers of Takanishi[9] and Lee and Liao.[10] At the end of the eighties Raibert and Thompson[11] studied the additional exploitation of natural dynamics of the hip motion by placing a torsional spring. At the same time McGeer (1990) built and studied a passive walker without compliant elements. Later he analysed it theoretically and by means of simulation walkers with hip compliance but with the body being a point-mass. During the nineties the group of Andy Ruina[12] studied in more detail the models of McGeer and extended the two dimensional model to three dimensions while building several Passive Walkers. In the second half of the nineties Ahmadi and Buehler[13] built a legged hopping monoped following the examples of Raibert using electrical actuation combined with a torsional spring in the hip and a linear spring in the telescopic leg. The control strategy was to calculate the passive dynamic trajectories with the correct initial conditions as a function of the desired forward speed, while in parallel with these trajectories standard active control was used to cope with imperfections of the modelling of the passive dynamics. A more intuitive control, but still focussing on exploiting natural dynamics, was done at MIT by Pratt et al. making use of the "Series Elastic Actuators".[14] These devices were used for the two legged "Spring Flamingo"[15] and consist of a motor drive in series with a linear elastic element. After 2000, Quartet III[16] was built by Osuka et al.; this quadruped starts walking down a sloped surface in an active way and gradually decreases control input to transfer to passive walking. Asano and Yamakita[17] introduced the "virtual gravity field" for horizontal walking in order to exhibit virtual passive walking based on McGeers models but with hip and ankle actuation. Wisse and van der Linde[18] studied a 3D Passive Walker with a pelvic body at the university of Delft (The Netherlands).

Most of these models use only the inertial properties to determine the *eigenfrequency* and additionally fixed compliance of mechanical linear or rotational springs. As a result, the *eigenfrequency* of these systems is set during construction which limits the different passive walking patterns and walking speeds. Flexibility, with the ability to change this natural frequency, is increased by implementing passive elements with variable compliance. In this context the group of Takanishi developed the two-legged walker WL-14,[19] where a complex non-linear spring mechanism makes changes in stiffness possible. A more elegant way to implement variable compliance is to use pneumatic artificial muscles, where the applied pressures determine stiffness. Research on this topic was done by Van der Linde,[20] Wisse,[21] Caldwell[22] and the Shadow Robot Company[23] by the implementation of McKibben muscles.

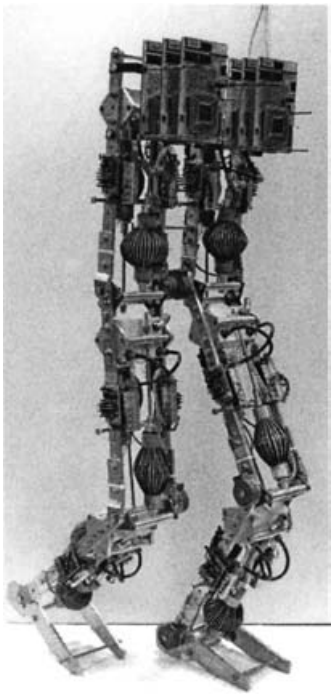


Fig. 1. Photograph of Lucy.

I.2. The biped lucy

Our research group Multi-body Mechanics of the Vrije Universiteit Brussel has built the planar walking biped Lucy. This biped model is actuated by pleated pneumatic artificial muscles (PPAM) which are a type of artificial muscle developed in our laboratory.[24] It gives an alternative to the McKibben type muscle by trying to overcome some of the latter's shortcomings such as a high threshold of pressure and dry friction. The goal of the biped project is to achieve a lightweight bipedal robot able to walk in a dynamically stable way, while exploiting the passive behaviour of the pleated pneumatic artificial muscles in order to reduce energy consumption and control efforts.

Figure 1 shows the complete robot Lucy which weighs, all included, less than 30 kg and is 150 cm tall. The motion of Lucy is restricted to the sagittal plane in order to avoid extra unnecessary complexity regarding control and design. Key elements in the design phase were modularity and flexibility regarding the ability to make changes to the robot configuration during the experimental process. This resulted in nearly the same mechanical and electronic configuration for each structural element, such as lower leg, upper leg and body.

The control philosophy intended for Lucy is to combine trajectory control based on objective parameters[25] with the natural dynamics of the system. More precisely, the natural dynamics of the system will be adapted in function of the objective parameters and the calculated joint trajectories based upon these parameters. This implies that a tool is needed to change the natural frequency of the system on-line, while an actuator should be able to track the desired trajectories. The pleated pneumatic artificial muscle, in an antagonistic set-up, is an actuator able to track trajectories, while its adaptable passive behaviour can be adjusted in order

https://doi.org/10.1017/S0263574704000669 Published online by Cambridge University Press

to change the natural dynamics by means of compliance variations in the different joints. This concept will be discussed in the paper.

II. REVOLUTE JOINT WITH THE PLEATED PNEUMATIC ARTIFICIAL MUSCLES

II.1. Pleated pneumatic artificial muscle: concept and characteristics

A pneumatic artificial muscle is essentially a membrane that will expand radially and contract axially when inflated, while generating high pulling forces along the longitudinal axis.

Different designs have been developed. The best known is the so called McKibben muscle.[26] This muscle contains a rubber tube which will expand when inflated, while a surrounding netting transfers tension. Hysteresis, due to dry friction between the netting and the rubber tube, makes control of such a device rather complicated. Typical of this type of muscle is a threshold level of pressure before any action can take place. The main goal of the new design[27,28] was to avoid friction, thus making control easier while avoiding the threshold. This was achieved by arranging the membrane into radially laid-out folds that can unfurl free of radial stress when inflated. Tension is transferred by stiff longitudinal fibres that are positioned at the bottom of each crease. A photograph of the inflated and deflated state of the Pleated Pneumatic Artificial Muscle (PPAM) is given in figure 2. If we omit the influence of elasticity of the high tensile strength material used for the fibres, the characteristic for the generated force is given by:

$$F = pl^2 f\left(\epsilon, \frac{l}{R}\right) \tag{1}$$

where p is the applied gauge pressure, l the muscle's full length, R its unloaded radius and ϵ the contraction.

The dimensionless function f, which depends only on contraction and geometry, is given for different values of broadness R/l in figure 3. The thicker the muscle, the less it contracts and the higher the forces it generates. Contraction can reach up to 54% in a theoretical case with $R/l = 0$.

A low contraction, forces are extremely high causing excessive material loading, and the generated forces drop too low for large contraction. Thus contraction will be bounded between two limits, 5 and 35% in practice. Figure 4 gives the generated force for different pressures of a muscle with initial length 10 cm and unloaded diameter 2.5 cm. Forces up to 3000 N can be generated with gauge pressure of only 300 kPa while the device weighs about 100 g.

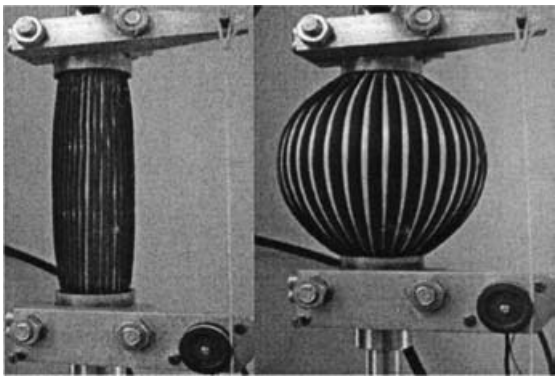


Fig. 2. Photograph of deflated and inflated state of the PPAM.

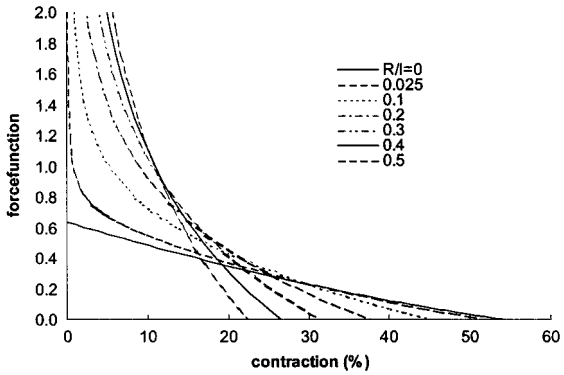


Fig. 3. Dimensionless force function.

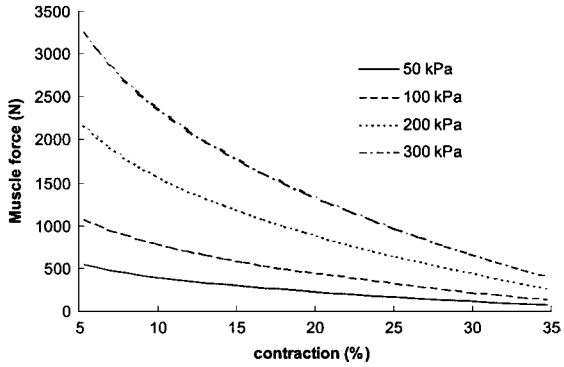


Fig. 4. Generated forces (N).

The graphs shown are derived from a mathematical model which fits experimental results with deviations of less than a few percent. This mathematical model will be of great importance for the design process of the different joints. Once the broadness is chosen and the pressure limits are set at 300 kPa to 400 kPa, in order to protect the membrane, an important design factor will be the length of the muscle. Expression (1) shows that the generated force is proportional to l squared.

II.2. Creating a revolute joint

Design and characteristics. Pneumatic artificial muscles can only pull. In order to have a bidirectionally working revolute joint one has to couple two muscles antagonistically. The muscle connections-pull rods and lever mechanism were designed so that the muscle's highly non-linear force-length characteristic is transformed into a more flattened torque-angle characteristic. Figure 5 shows the straightforward connecting principle.

Depending whether the joint is a knee, ankle or hip the dimensions can be chosen in order to meet the needs of the specified joint function, not only at torque levels but also in range of motion which is different for an ankle and a knee.

https://doi.org/10.1017/S0263574704000669 Published online by Cambridge University Press

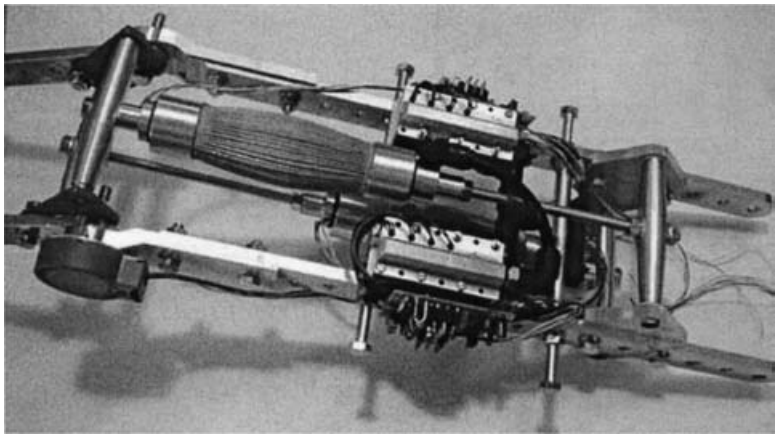


Fig. 5. Photograph of the two dimensional rotative joint.

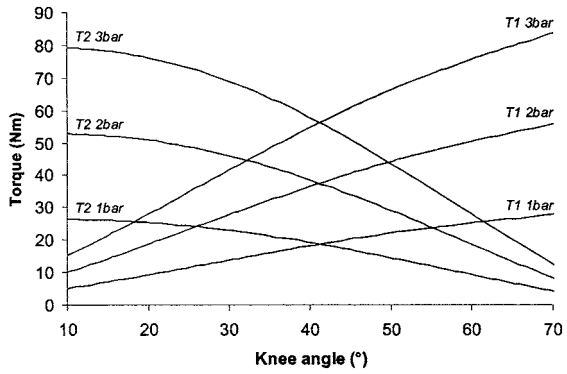


Fig. 6. Knee torques.

As an example, Figure 6 gives the knee torque characteristics chosen for LUCY.

Here T_1 is the extensor muscle torque and T_2 the torque generated by the flexor muscle. Both torques are given for different pressure values. If the knee is stretched the knee angle has the value zero.

Taking into account equation (1) and if r_1 and r_2 define the leverage arm of the extensor and flexor muscle respectively, the joint torque is given by following expression

$$\begin{aligned} T = T_1 - T_2 &= p_1 l_1^2 r_1 f_1 - p_2 l_2^2 r_2 f_2 \\ &= p_1 t_1(\theta) - p_2 t_2(\theta) \end{aligned} \qquad (2)$$

with p_1 and p_2 the applied gauge pressures in extensor and flexor muscles, respectively, which have lengths l_1 and l_2. The dimensionless force functions of both muscles are given by f_1 and f_2. The functions t_1 and t_2, in equation (2), are determined by the choices made during the design phase and depend on the knee angle θ. Thus the joint position is influenced by weighted differences in gauge pressures of both muscles. Note that equation (2) is valid in case that the inertial properties of muscle membrane and attachments are neglected.

Pressure control. Pneumatic artificial muscles have a high power-to-weight ratio which makes them suitable for legged robots. But for a pneumatic system, a pressure control device should be taken into account to evaluate this ratio if the valve system is included on board of the robot. So the weight of the valves controlling the muscles should be chosen as low as possible. But since most pneumatic systems are designed for fixed automation purposes, where weight is not an issue at all, most off-the-shelf proportional valves are far to heavy for this application. Thus a proper design of the pressure control is of great importance.

In order to realize a lightweight rapid and accurate pressure control, fast switching on-off valves are used. The pneumatic solenoid valve 821 2/2 NC made by Matrix weighs only 25 g. With their reported opening times of about 1 ms and flow rate of 180 Std.1/min, they are about the fastest switching valves of that flow rate currently available.

To pressurize and depressurize the muscle which has a varying volume up to 400 ml, it is best to place a number of these small on-off valves in parallel. Obviously, the more valves used the higher electric power consumption, price and weight will be. Simulations of the pressure control of a constant volume lead to the compromise of two inlet and four outlet valves. The different number between inlet and outlet arises from the asymmetric pressure conditions between these two combined with the aim to create equal muscle's inflation and deflation times. The six valves were brought together in a valve island with special designed inlet and outlet collectors after removing useless original housing material. The weight of this device is less than 150 g.

The pressure control in a volume is achieved with a bang-bang controller with various reaction levels depending on the pressure error. If this error is large the two inlet or the four outlet valves, depending on the sign of the error, are switched together. If this error is smaller, only one valve will be switched and when the error is within reasonable limits no action will be taken leaving the muscle closed. The principle of this control scheme is depicted in figure 7. More detailed information on the valve system can be found in reference [29].

II.3. Adaptable passive behaviour of a revolute joint

The PPAM has two sources of compliance: gas compressibility and the dropping force to contraction characteristic.[24] The latter effect is typical for pneumatic artificial muscles, while the first is similar to standard pneumatic cylinders.

https://doi.org/10.1017/S0263574704000669 Published online by Cambridge University Press

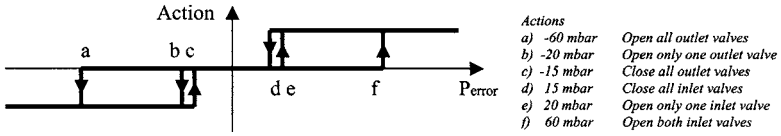


Fig. 7. Multi-level bang-bang control scheme.

Joint stiffness, the inverse of compliance, for the considered revolute joint can be obtained by the angular derivative of the torque characteristic in equation (2):

$$K = \frac{dT}{d\theta} = \frac{dT_1}{d\theta} - \frac{dT_2}{d\theta} = \frac{dp_1}{d\theta} t_1 + p_1 \frac{dt_1}{d\theta} - \frac{dp_2}{d\theta} t_2 - p_2 \frac{dt_2}{d\theta} \tag{3}$$

The terms $dp_i/d\theta$ represent the share in stiffness of changing pressure with contraction, which is determined by the action of the valves controlling the joint and by the thermodynamic processes taking place. If the valves are closed and if we assume polytropic compression/expansion the pressure changes inside the muscle will be a function of volume changes:

$$P_i V_i^n = P_{i_o} V_{i_o}^n \tag{4}$$

with:

$$P_i = P_{atm} + p_i \tag{5}$$

leading to:

$$\frac{dp_i}{d\theta} = -n\left(P_{atm} + p_{i_o}\right) \frac{V_{i_o}^n}{V_i^{n+1}} \frac{dV_i}{d\theta} \tag{6}$$

With P_i, V_i the absolute pressure and volume of muscle i, P_{i_o} the absolute initial pressure, V_{i_o} the initial volume when muscle i was closed and p_i, p_{i_o} the gauge pressure and initial gauge pressure. n is the polytropic index and P_{atm} the atmospheric pressure.

Taking the knee characteristics as an example, the following reasoning can be made for closed muscles. An increase of the knee angle θ— bending the leg — will result in an increase of the torque generated by the extensor muscle (see figure 6) while its volume will decrease. Thus $dt_1/d\theta > 0$ and $dV_1/d\theta < 0$. For the flexor muscle the actions will be opposite to this. Combining equation (3), (4) and (6) with this information gives:

$$K = \left(k_1 p_{1_o} + k_2 p_{2_o} + k_{atm} P_{atm}\right) \tag{7}$$

with:

$$k_1 = t_1 n \frac{V_{1_o}^n}{V_1^{n+1}} \left|\frac{dV_1}{d\theta}\right| + \frac{V_{1_o}^n}{V_1^n} \left|\frac{dt_1}{d\theta}\right| > 0$$

$$k_2 = t_2 n \frac{V_{2_o}^n}{V_2^{n+1}} \left|\frac{dV_2}{d\theta}\right| + \frac{V_{2_o}^n}{V_2^n} \left|\frac{dt_2}{d\theta}\right| > 0$$

$$k_{atm} = k_1 + k_2 - \left|\frac{dt_1}{d\theta}\right| - \left|\frac{dt_2}{d\theta}\right|$$

The coefficients k_1, k_2, k_{atm} are a function of the angle and are determined by the geometry parameters of the joint and muscles. From equation (7) the conclusion is drawn that a passive spring element is created with an adaptable stiffness controlled by the weighted sum of both initial gauge pressures when closing the muscle.

Since stiffness depends on a sum of gauge pressures while position is determined by differences in gauge pressure (see subsection on Design and Characteristics), the angular position can be controlled while setting stiffness.

III. AN EXAMPLE OF TRAJECTORY CONTROL WITH ADAPTED COMPLIANCE

The purpose of this section is to illustrate the proposed strategy of combining adaptable passive behaviour with trajectory control. Moreover, the effect on control activity and energy consumption by changing compliance characteristics will be shown on a simplified model of a leg. For this model only the knee is actuated.

Exploitation of the natural dynamics with changing compliance characteristics can be seen from two points of view. One can let the system oscillate at its natural frequency and adapt this frequency by changing the joint compliance to alter motion characteristics. But this limits the flexibility towards different desired motion patterns. Or one can impose a desired joint trajectory which corresponds to the desired global motion of the system. And, subsequently, an appropriate joint compliance can be selected so that the base frequency components of the movements corresponding to the natural dynamics approach the base frequency of the imposed joint trajectory. Doing so will reduce control activity of the joint trajectory tracking controller. It is the latter principle that will be shown in this section.

III.1. Description of the setup

The geometry of this model is given in figure 8 while the inertial parameters are given in table I. The leg consists of three parts: lower leg, upper leg and body. The Hip (**H**) and Foot (**F**) are attached to a vertical slider and the body is modelled as a point mass. The knee (**K**) is powered by the joint mechanism as described in section II.2. The length of the i-th link is l_i, its mass is m_i and the moment of inertia about its center of mass G_i is I_i. The location of the center of mass G_1 of the lower leg and G_2 of the upper leg are

Table I. Inertial parameters of the leg model.

i	$l_i\,(m)$	$m_i\,(kg)$	$I_i\,(kgm^2/s)$
1	0.4	2	0.0138
2	0.4	3.5	0.0218
3	/	10	/

https://doi.org/10.1017/S0263574704000669 Published online by Cambridge University Press

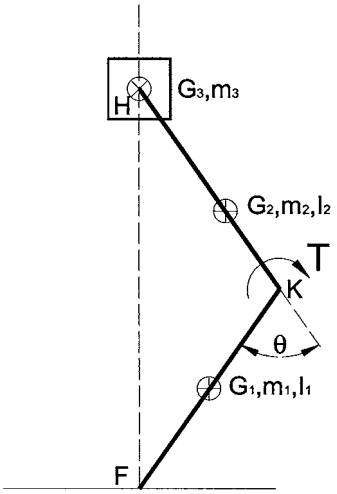


Fig. 8. Schematic overview of the studied model.

given by $FG_1 = \alpha l_1, KG_2 = \beta l_2$ with $0 < \alpha, \beta < 1$. For this simulation $\alpha = \beta = 0.5$.

When assuming a continuous contact without slip of the foot with the ground, this model has one degree of freedom which is represented by the relative knee angle θ.

III.2. Simulation model

The proposed strategy will be illustrated by means of a simulation. The differential equations for this simulation can be divided into two parts: Firstly, the mechanical part representing the motion of the leg in the gravity field by application of the knee torque T. And, secondly, the pneumatic part describing the thermodynamic processes for the two muscle-valve systems. These processes will determine the pressure evolutions in both muscles and consequently the exerted knee torque.

Mechanics. If the joints are assumed to be frictionless, the equation of motion describing the motion of the leg due to the applied knee torque will be given by (appendix A):

$$M(\theta)\ddot{\theta} + C(\theta, \dot{\theta})\dot{\theta} + G(\theta) = T \tag{8}$$

with:

$$M(\theta) = \frac{1}{4}(I_1 + I_2 + m_1\alpha^2 L^2 + m_2(1+\beta^2)L^2 + 2m_3 L^2 - 2L^2(m_2\beta + m_3)\cos\theta) \tag{9}$$

$$C(\theta, \dot{\theta}) = \frac{1}{4}L^2((m_2\beta + m_3)\sin\theta)\dot{\theta} \tag{10}$$

$$G(\theta) = -g\frac{L}{2}(\alpha m_1 + (1+\beta)m_2 + 2m_3)\sin\frac{\theta}{2} \tag{11}$$

This equation holds for identical length L of upper and lower leg which is in accordance with table I. The gravitational acceleration is represented by g and the torque T, provided by the antagonistic setup, is given by equation (2).

Pneumatics. The pressure inside a muscle will be influenced by the volume changes resulting from the variation of the knee angle and by the orifice flows through the valves which have been activated by the bang-bang controller. Assuming a polytropic thermodynamic process, and the compressed air inside each muscle to behave as a perfect gas, the first law of thermodynamics, while neglecting the fluid's kinetic and potential energy, can be rewritten in the following form:[24]

$$\dot{p}_1 = \frac{n}{V_1}\left(rT^{in}\dot{m}_1^{in} - rT_1\dot{m}_1^{ex} - (P_{atm} + p_1)\dot{V}_1\right) \tag{12}$$

$$\dot{p}_2 = \frac{n}{V_2}\left(rT^{in}\dot{m}_2^{in} - rT_2\dot{m}_2^{ex} - (P_{atm} + p_2)\dot{V}_2\right) \tag{13}$$

with r the dry air gas constant and n the polytropic index. T^{in} is the temperature of the supply air and T_i the temperature in muscle i. The total orifice flow through the opened inlet valves and exhaust valves of muscle i are given respectively by $\dot{m}_i^{in}$ and $\dot{m}_i^{ex}$. The latter two can be calculated with following equations which is the normalized approximation of a flow through a valve defined by ISO6358 [30]:

$$\dot{m} = CP_u\rho_0\sqrt{\frac{293}{T_u}}\sqrt{1-\left(\frac{P_d/P_u - b}{1-b}\right)^2} \quad \text{if} \quad \frac{P_d}{P_u} \geq b \tag{14}$$

$$\dot{m} = CP_u\rho_0\sqrt{\frac{293}{T_u}} \quad \text{if} \quad \frac{P_d}{P_u} \leq b \tag{15}$$

with ρ_0 the air density at standard conditions. C and b are two flow coefficients characterizing the valve. Both coefficients have been experimentally determined for the matrix valves which resulted in $C = 22$ Std.l/min bar and $b = 0.16$. P_u and P_d are the upstream and downstream pressures while T_u is the temperature upstream. When choking occurs equation (15) is valid, in the other case equation (14) is used.

Once the actions (opening of the valves) for the different inlet and exhaust valves are known, all the orifice flows can be calculated in order to be substituted in (12) and (13). To simulate the leg motion these two equations will be integrated together with the perfect gas law and the equation of motion (8) while using the kinematic expression (2) to replace torque T.

Complete low-level joint controller. In order to perform the integration of the simulation model discussed in the former paragraph the activations of the different on/off valves has to be known. This valve activation depends on the design of the low-level controller and is determined by the desired trajectory. But when using pneumatic artificial muscles the mean pressure of both muscles in the antagonistic set-up is a third important influencing factor. The considered controller is given in the schematic overview of figure 9. This low-level controller can be divided in three parts: the feedback linearization module,[31] the inverse delta-p unit and the bang-bang controller discussed in subsection on Pressure Control (II.2).

In the first module the computed torque T is composed of the feed-forward term $M(\theta)\ddot{\theta}_{des}$, the centrifugal/gravitational compensation term $C(\theta, \dot{\theta})\dot{\theta} + G(\theta)$ and a proportional and derivative feedback part for which the gains are tuned in order for the mechanical system to behave critically damped.

https://doi.org/10.1017/S0263574704000669 Published online by Cambridge University Press

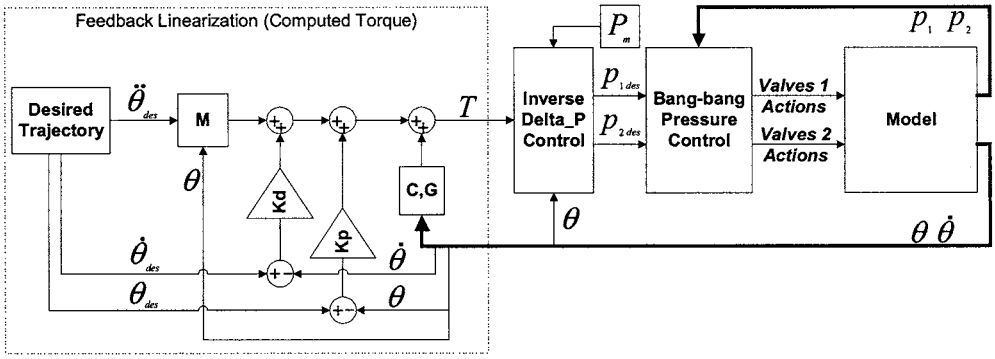


Fig. 9. The applied low-level control scheme.

The computed torque is then feeded into the inverse delta-p control unit which calculates the necessary pressure values to be set in the muscles. These two gauge pressures are generated from a mean pressure value p_m while adding and subtracting a Δp value:

$$p_1 = p_m + \Delta p \tag{16}$$

$$p_2 = p_m - \Delta p \tag{17}$$

Feeding back the knee angle θ and using expression (2), Δp can be determined by:

$$\Delta p = \frac{T + p_m((t_2(\theta) - t_1(\theta))}{t_2(\theta) + t_1(\theta)} \tag{18}$$

The delta-p unit is actually a feed-forward calculation from torque level to pressure level using the kinematic model of the muscle actuation system. The calculated Δp affects the torque needed to follow the desired trajectory while p_m is introduced to determine the sum of pressures which influences the stiffness of the joint as was discussed in section II.3. Increasing p_m will lower the compliance of the joint. Note that this control law does not decouple stiffness control from position control since the weights k_1 and k_2 (see section III.3) are not taken into account. But for this example the stiffness (chosen with p_m) will be set at a fixed value at the beginning of each simulation.

In the last control block the desired gauge pressures calculated by the delta-p unit are compared with the measured gauge pressure values after which appropriate valve actions are taken by the bang-bang pressure controller. The opening and closing of the valves will eventually determine the motion of the leg.

The simulation model takes into account the delay time of about 1 ms for the valves as was mentioned in section II.2 (subsection on Pressure Control) and incorporates a sampling rate of 500 Hz, which means that the control-unit updates the actions to be taken by the valves every 2 ms.

III.3. Simulation results and discussion

With pressurized closed muscles and taken out of its static balance position the leg will start to oscillate at its natural frequency when released. This frequency will depend on the mean pressure and on the initial conditions from which the mechanism is launched due to the non-linearity of the system. If this passive trajectory would be the desired trajectory, no valve switching would be necessary if the compliance and initial conditions where the same. Increasing or decreasing the mean pressure in this situation will result in more control activity and consequently pneumatic power consumption. When, on the other hand, imposing an arbitrary trajectory such as a sinewave of a certain frequency, it will not be possible to track this without valve switching since the natural trajectory does not fit exactly. But it will then be important to select an appropriate mean pressure in order to reduce control activity. This will be shown with the following two simulation results.

A knee trajectory, a sine of 2 Hz and displacement of 0.6 rad to 0.8 rad, will be simulated in a first run at $p_m = 1$ bar and in a second run at $p_m = 2$ bar. The results shown represent one period with initial pressures and torques calculated dynamically to fit the sine-wave. For each simulation, desired and measured pressures and valve actions for both muscles are shown. Figures 10 and 11 show a simulation with 1 bar mean pressure while figures 12 and 13 are the results of a simulation with 2 bar mean pressure. The accumulated tracking error for both simulation with 1 bar and 2 bar mean pressure are, respectively, 1.07 10^{-4} rad and 0.87 10^{-4} rad, which are comparable.

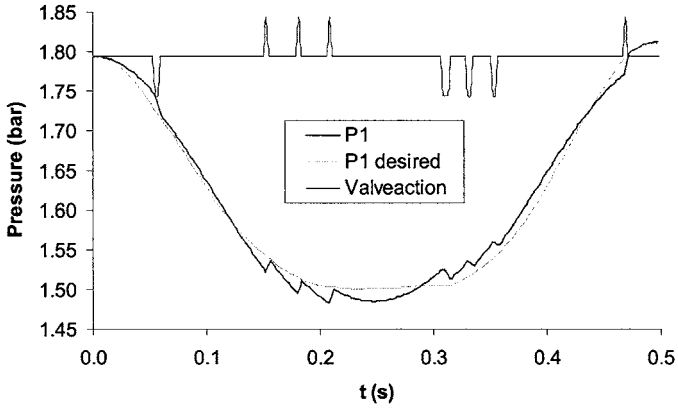


Fig. 10. Desired and measured pressure in muscle 1 for a mean pressure value of 1 bar.

https://doi.org/10.1017/S0263574704000669 Published online by Cambridge University Press

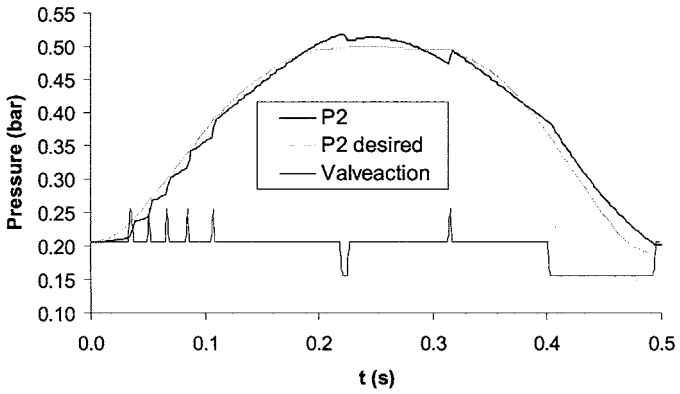


Fig. 11. Desired and measured pressure in muscle 2 for a mean pressure value of 1 bar.

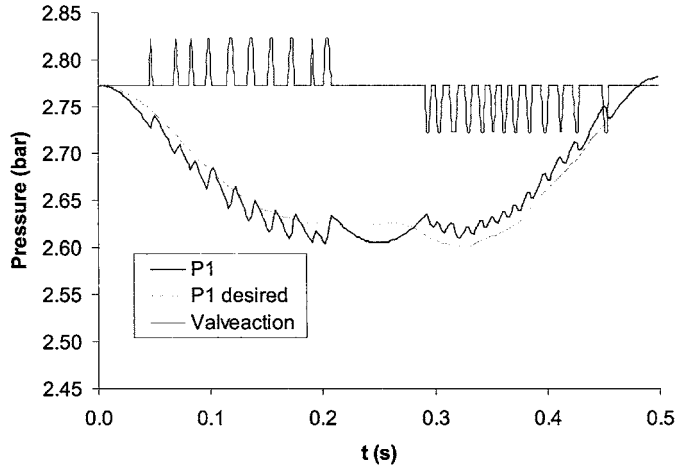


Fig. 12. Desired and measured pressure in muscle 1 for a mean pressure value of 2 bar.

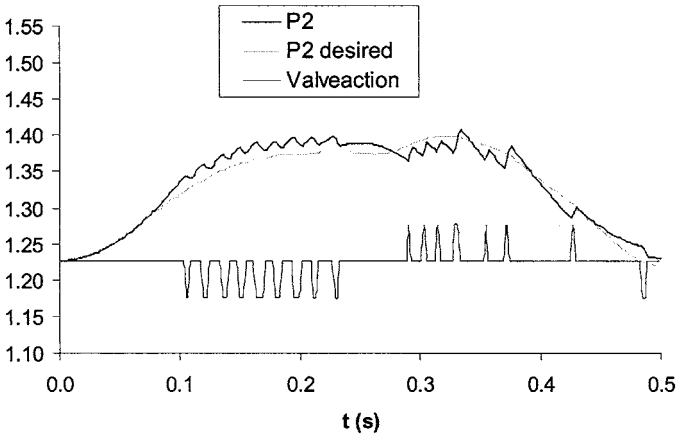


Fig. 13. Desired and measured pressure in muscle 2 for a mean pressure value of 2 bar.

Note that in these figure a closed muscle is represented by a horizontal line depicted at the same level of the initial pressure, while a peak upwards represents one opened inlet valve, a peak downwards one opened exhaust valve. Only one inlet or exhaust valve is switching.

Comparing the valve actions taken for both simulations, it is clearly seen that 1 bar mean pressure is more suited to track a sine-wave of two hertz. The control activity in the case of 2 bar mean pressure is remarkably higher. For example, at the graph in figure 10 it is seen that no valve action is taken between 0.06 s and 0.14 s because the slope of the pressure values induced by the natural dynamics fits the one of the desired pressure needed to follow the sine-wave. Contrary to these results, for the same time interval on the graph in figure 12 for which opening of the inlet valve is each time needed to compensate the pressure drop, with closed muscles, which is too high compared to the desired pressure course.

Calculation of the pneumatic energy input via the inlet valves, while neglecting kinetic and potential fluid energy and taking reference at $T = 0$, is given by:

$$E^{in}_{pneu} = \int C_p T^{in} dm^{in} \tag{19}$$

with C_p the specific heat at constant pressure, T^{in} the temperature of the supply air and dm^{in} the sum of both inlet orifice mass flows. For the case of 1 bar mean pressure, this results in 17.76 J for the complete period, while in the other case the pneumatic energy input is more than doubled to a value of 41.80 J!. Note that this simulation does not give the lowest energy consumption values since the characteristics of the muscles are those taken for the biped Lucy. This example is given to demonstrate the importance of selecting the appropriate mean pressure in order to adapt the natural dynamics in function of the desired trajectory. Furthermore, it should be remarked that the total dynamic behaviour and also the way in which the natural dynamics are exploited will strongly depend on design of the control unit and its parameters. For example, changing the reaction levels of the bang-bang controller will influence the valve switching. Decreasing these levels and increasing the bandwidth of the feedback controller will increase valve switching and consequently pneumatic energy consumption. This leads to the ever returning compromise between energy consumption and tracking error.

IV. CONCLUSIONS

In this paper the important feature of adapting the natural dynamics by using pneumatic artificial muscles was discussed. The Pleated Pneumatic Artificial Muscle and its force characteristics were introduced together with the one-dimensional rotative joint module used for the biped Lucy. This rotative mechanism is driven by two straightforward antagonistically connected muscles for which it was shown that pressure differences determine position, while the sum of pressures in both muscles influences the stiffness of the joint. This mean pressure will influence the natural frequency of the system which should be selected in function of the desired trajectory. To show the importance of selecting the appropriate value regarding energy consumption and control activity an elaborate simulation model was built and results were shown. Future work will be the incorporation of the mean pressure value determination in a higher-level control

https://doi.org/10.1017/S0263574704000669 Published online by Cambridge University Press

strategy. Experiments on the real physical model Lucy will accompany the simulation results.

Acknowledgement
The third author B. Vanderborght is PhD student with a grant from the Fund for Scientific Research-Flanders (Belgium) (FWO). Lucy has been built with the financial support of the Research Council (OZR) of the Vrije Universiteit Brussel.

References

1. K. Hirai, M. Hirose, Y. Haikawa and T. Takenaka, "The development of honda homanoid robot," *IEEE International Conference on Robotics and Automation*, Leuven, Belgium, (1998) pp. 1321–1326.
2. Sony-PressRelease, *World's first running humanoid robot* (December 18th, 2003).
3. Y. Kuroki, T. Ishida, J. Yamagushi, M. Fujita and T. Doi, "A small biped entertainment robot," *IEEE-RAS International Conference on Humanoid Robots* (2001) pp. 184–186.
4. K. Yokoi et al., "Humanoid robot's applications in HRP," *IEEE International Conference on Humanoid Robots*, Karlsruhe, Germany (2003).
5. F. Pfeiffer, K. Löffler and M. Gienger, "Sensor and control aspects of biped robot "johnnie"," *IEEE International Conference on Humanoid Robots*, Munich, Germany (2003).
6. M. A. Diftler and R. Ambrose, "ROBONAUT, a robotic astronaut assistant," *ISAIRAS Conference*, Montreal, Canada (2001) pp. 179–197.
7. K. Matsuoka, "A mechanical model of repetitive hopping movements," *Biomechanics* **5**, 251–258 (1980).
8. M. Raibert, *Legged Robots That Balance* (Cambridge, Massachussetts: MIT Press, 1986).
9. A. Takanishi, M. Ishida, Y. Yamazaki and I. Kato, "The realization of dynamic walking by the biped walking robot wl-10rd," *Proceedings International Conference on Advanced Robotics*' **85**, (1985) pp. 459–466.
10. T.-T. Lee and J.-H. Liao, "Trajectory planning and control of a 3-link biped robot," *Proceedings IEEE International Conference on Robotics and Automation*, New York, USA, (1988) pp. 820–823.
11. C. Thompson and M. Raibert, "Passive dynamic running," *Proceedings International Symposium of Experimental Robotics* (V. Hayward and O. Khatib, eds.) (Springer-Verlag, 1989) pp. 74–83.
12. M. Garcia, A. Chatterjee, A. Ruina and M. Coleman, "The simplest walking model: Stability, complexity, and scaling," *ASME Journal of Biomechanical Engineering* **120**, 281–288 (1988).
13. P. Gregorio, M. Ahmadi and M. Buehler, "Design, control, and energetics of an electrically actuated legged robot," *IEEE Transactions on Systems, Man, and Cybernetics* **27B**, 626–634 (August, 1997).
14. G. A. Pratt and M. M. Williamson, "Series elastic actuators," *Proceedings IEEE-IROS Conference*, Pittsburg, USA, (1995) pp. 399–406.
15. J. E. Pratt and G. Pratt, "Exploiting natural dynamics in the control of a planar bipedal walking robot," *36th annual Allerton Conference on Communication, Control, and Computing*, Monticello, Illinois (1988) pp. 739–748.
16. K. Osuka and Y. Saruta, "Development and control of new legged robot QUARTET III-from active walking to passive walking," *Proceedings of the 2000 IEEE/RSJ International Conference on Intellegent Robots and Systems* (2000) pp. 991–995.
17. F. Asano, M. Yamkita and K. Furuta, "Virtual passive dynamic walking and energy-based control laws," *Proceedings of the IEEE/RSJ International Conference on Intelligent Robots and Systems (IROS), IEEE/RSJ* (2000) **Vol 2**, pp. 1149–1154.
18. M. Wisse, A. L. Schwab and R. Q. vd. Linde, "A 3d passive dynamic biped with yaw and roll compensation," *Robotica* **19**, Part 3, 275–284 (2001).
19. J. Yamguschi, D. Nishino and A. Takanishi, "Realization of dynamic biped walking varying joint stiffness using antagonistic driven joints," *IEEE International Conference on Robotics and Automatisation*, Leuven, Belgium (1998) pp. 2022–2029.
20. R. Q. V. der Linde, "Active legcompliance for passive walking," *IEEE International Conference on Robotics and Automatisation* (1998) pp. 2330–2344.
21. M. Wisse, "Biologically inspired biped design," *Symposium of the Int. Soc. For Postural and Gait Research*, Maastricht, The Netherlands (2001) pp. 900–903.
22. S. T. Davis and D. G. Caldwell, "The bio-mimetic design of a robot primate using pneumatic muscle actuators," *CLAWAR 2001: Proceedings of the 4th International Conference on Climbing and Walking Robots*, Karlsruhe, Germany (Professional Engineering Publishing, 2001) pp. 197–204.
23. http://www.shadow.org.uk
24. F. Daerden, "Conception and Realization of Pleated Pneumatic Artificial Muscles and their Use as Compliant Actuation Elements," *PhD thesis* (Vrije Universiteit Brussel, Brussels, 1990).
25. J. Vermeulen, D. Lefeber and B. Verrelst, "Control of foot placement, forward velocity and body orientation of a one-legged hopping robot," *Robotica* **21**, Part 1, 45–57 (2003).
26. H. F. Schulte, "The characteristics of the McKibben artificial muscle," **In**: *The Application of External Power in Prosthetics and Orthotics*, No. Publication 874 (Lake Arrowhead: National Academy of Sciences-National Research Council, 1961) pp. 94–115.
27. F. Daerden and D. Lefeber, "The concept and design of pleated pneumatic artificial muscles," *International Journal of Fluid Power* **2**, No. 3, 41–50 (2001).
28. F. Daerden, D. Lefeber, B. Verrelst and R. Van Ham, "Pleated pneumatic artificial muscles: actuators for automation and robotics," *IEEE/ASME International Conference on Advanced Intellegent Mechatronics*, Como, Italy (2001). pp. 738–743.
29. R. Van Ham, F. Daerden, B. Verrelst, D. Lefeber and J. Vandenhoudt, "Control of pneumatic artificial muscles with enhanced speed up circuitry," *CLAWAR 2002: 5th International Conference on Climbing and Walking Robots*, Paris, France (2002) pp. 195–202.
30. International Standard ISO6358, "Pneumatic fluid power – method of test – determination of flow rate characteristics of components using compressible fluids," (1989).
31. J. J. E. Slotine and W. Li, *Applied Nonlinear Control* (Cambridge, MA.: Prentice-Hall, 1991).

APPENDIX A: MECHANICAL MODELISATION

In this section the equation of motion used in paragraph III.2 (subsection on mechanics) will be derived with the Newton-Lagrange formulation:

$$\frac{d}{dt}\left\{\frac{\partial K}{\partial \dot{\theta}}\right\} - \frac{\partial K}{\partial \theta} + \frac{\partial U}{\partial \theta} = Q_\theta \tag{20}$$

Here K is the total kinetic energy and U the gravitational potential energy. Q_θ is the generalized force of the knee which in this case is represented by the torque T.

The total kinetic energy of the model and its derivatives are given by:

$$K = \frac{1}{8}(I_1 + I_2 + m_1\alpha^2 L^2 + m_2(1+\beta^2)L^2 + 2m_3L^2 - 2L^2(m_2\beta + m_3)\cos\theta)\dot{\theta}^2$$

https://doi.org/10.1017/S0263574704000669 Published online by Cambridge University Press

$$\frac{d}{dt}\left\{\frac{\partial K}{\partial \dot{\theta}}\right\} = \frac{1}{4}(I_1 + I_2 + m_1\alpha^2L^2 + m_2(1+\beta^2)L^2 + 2m_3L^2 - 2L^2(m_2\beta + m_3)\cos\theta)\ddot{\theta} + \frac{1}{2}L^2((m_2\beta + m_3)\sin\theta)\dot{\theta}^2 \quad (21)$$

$$\frac{\partial K}{\partial \theta} = \frac{1}{4}L^2((m_2\beta + m_3)\sin\theta)\dot{\theta}^2 \quad (22)$$

The gravitational potential energy and its partial derivative are calculated as:

$$U = gL(\alpha m_1 + (1+\beta)m_2 + 2m_3)\cos\frac{\theta}{2}$$

$$\frac{\partial U}{\partial \theta} = -g\frac{L}{2}(\alpha m_1 + (1+\beta)m_2 + 2m_3)\sin\frac{\theta}{2} \quad (23)$$

Substituting (21), (22) and (23) in (20) gives the equation of motion which can be summarized in the following form:

$$M(\theta)\ddot{\theta} + C(\theta,\dot{\theta})\dot{\theta} + G(\theta) = T$$

with:

$$M(\theta) = \frac{1}{4}(I_1 + I_2 + m_1\alpha^2L^2 + m_2(1+\beta^2)L^2 + 2m_3L^2 - 2L^2(m_2\beta + m_3)\cos\theta)$$

$$C(\theta,\dot{\theta}) = \frac{1}{4}L^2((m_2\beta + m_3)\sin\theta)\dot{\theta}$$

$$G(\theta) = -g\frac{L}{2}(\alpha m_1 + (1+\beta)m_2 + 2m_3)\sin\frac{\theta}{2}$$

https://doi.org/10.1017/S0263574704000669 Published online by Cambridge University Press